instruments

MDPI

Article

Niobium as Preferential Material for Cyclotron Target Windows

Sergio J. C. do Carmo [1,2] and Francisco Alves [2,3,*]

[1] ICNAS Pharma, Institute for Nuclear Sciences Applied to Health, University of Coimbra, 3000-548 Coimbra, Portugal; sergiocarmo@uc.pt
[2] CIBIT/ICNAS, Institute for Nuclear Sciences Applied to Health, University of Coimbra, 3000-548 Coimbra, Portugal
[3] Polytechnic Institute of Coimbra, Coimbra Health School, 3045-093 Coimbra, Portugal
* Correspondence: franciscoalves@uc.pt

Abstract: The present work promotes and validates the benefits of using niobium instead of Havar® as the material for the target windows in most routine irradiations in cyclotrons. Calculation of the material activation and measurements of the contamination of the transferred target liquids show major improvements with the use of niobium. Also, the data of the daily routine productions at our production center are presented, proving that Havar® is not mandatory unless large target currents and/or pressures are required.

Keywords: cyclotron; radioisotope production; targetry; niobium; target window

Citation: do Carmo, S.J.C.; Alves, F. Niobium as Preferential Material for Cyclotron Target Windows. *Instruments* **2024**, *8*, 33. https://doi.org/10.3390/instruments8020033

Academic Editor: Antonio Ereditato

Received: 23 April 2024
Revised: 16 May 2024
Accepted: 22 May 2024
Published: 27 May 2024

1. Introduction

The use of niobium in cyclotron targetry is well established and has long been proven effective; this metal provides consistent advantages due to its chemical inertness, good thermal conductivity and high melting point, among other factors [1]. Also, niobium has a low activation cross-section for both protons and thermal neutrons, producing thus far less activation when compared to other suitable options—A characteristic particularly relevant for periodic maintenance tasks. Finally, the activation of niobium reduces drastically after a reduced cooling time, an advantage usually not provided by other materials such as silver.

Similar considerations are valid when considering the material for target windows. However, in this case, it is also mandatory to present improved mechanical strength, even with minimum thickness. For this particular reason, Havar®, over the years, he become the standard solution for target windows working at high currents and pressures. Unfortunately, this choice came at the expense of harmful consequences since (i) Havar®—like any steel alloy—presents a multitude of components and, therefore, several radiocontaminants; and (ii) its irradiation results in intense long-term activation.

As biomedical cyclotrons have been developed throughout recent decades for the optimized production of ^{18}F, with their main goal of the synthesis of ^{18}F-FDG borne in mind, these machines usually provide protons with a fixed energy of around 16–19 MeV, depending on the manufacturer. Although such an energy range is suitable for the production of ^{18}F, it is too high for the production of medically emergent radioisotopes (e.g., ^{68}Ga) [2]. The use of thicker target windows as degraders to reduce the initial energy of the beam on the target has therefore become frequent, with Havar® becoming much less adequate with larger thicknesses due to its inferior thermal conductivity leading to increased heat load. Moreover, the many (both cold and radioactive) metallic contaminants released from Havar® during irradiation—and leaching, especially, into liquid target material—are additionally prohibitive for radiolabeling processes involving radiometals, therefore making it mandatory to use a distinct material for target windows.

It is within this particular and more contemporary scenario that niobium naturally became considered as an alternative for target windows, not only because of the previously

mentioned advantages but also because the target cavity is usually already made of niobium. Its use for target windows therefore avoids the addition of new materials and/or contaminants—either cold or radioactive—within further processes. Furthermore, unlike Havar®, there is no longer a need for it to be treated as long-term radioactive waste since its activation decays massively after only 2–3 months. The eventual production of ^{93}Mo is the only exception [3], depending on the incident proton energy. Moreover, niobium is also more affordable and less dangerous (e.g., it contains no beryllium, unlike Havar®).

This work presents the benefits of using niobium for target windows, presenting those benefits in terms of the handling of radioactive waste and reduction of transferred radiocontamination, while simultaneously presenting performance data for reliable daily routine use with several thicknesses and distinct production routes.

2. Methods and Results

At the Institute of Nuclear Sciences Applied to Health (ICNAS) of the University of Coimbra, the cyclotron and radiochemistry laboratory operates daily for the production of radiopharmaceuticals for both routine productions and R&D activities based mainly on the radioisotopes ^{11}C, ^{13}N, ^{18}F, ^{61}Cu, ^{64}Cu, ^{68}Ga and ^{89}Zr. These latter are produced thanks to two cyclotrons from the manufacturer IBA, namely, the Cyclone 18/9 model, delivering 18 MeV protons and 9 MeV deuterons, and the Kiube Variable Energy cyclotron, delivering protons with energy ranging from 13 to 18 MeV. The cyclotron target systems used are either gaseous or liquid and require target windows made of aluminium, titanium, niobium or Havar®. Table 1 presents calculations for the cumulated production yields for the radioisotopes with half-lives greater than 2 weeks produced in these target windows of different materials with distinct thicknesses and irradiated at either 13 or 18 MeV. Some of these radioisotopes are even produced though several nuclear reaction routes (e.g., ^{57}Co is produced via the ^{59}Co(p,p2n)^{57}Co, ^{56}Fe(p,γ)^{57}Co, ^{57}Fe(p,n)^{57}Co, ^{58}Fe(p,2n)^{58}Co, ^{58}Ni(p,2p)^{57}Co and ^{60}Ni(p,α)^{57}Co reactions). The cumulated production yields were obtained using excitation curve fits from cross-section data available in the EXFOR database [4].

Table 1. Radioisotopes with half-lives greater than 2 weeks produced by proton irradiation at 18 and 13 MeV in the different target windows.

Radioisotope Produced	Half-Life	Cumulated Production Yield	Cross-Section Data	Estimation of Activation after One Month of Irradiation
	(months)	(MBq/μA_{sat})		(MBq)
500 µm thick aluminium irradiated at 18 MeV (for ^{14}N(p,α)^{11}C)				
^{22}Na	31.224	33.77	[5]	0.81
^{26}Al	8.60×10^{6}	1790.32	[6]	1.56×10^{-4}
12.5 µm thick titanium irradiated at 18 MeV (for ^{14}N(p,α)^{11}C, ^{18}O(p,n)^{18}F, ^{nat}Zn(p,n)^{61}Cu, and ^{64}Ni(p,n)^{64}Cu)				
^{48}V	0.525	69.46	[7,8]	757.27
^{46}Sc	2.7529	1.328	[8]	6.26
12.5 µm thick titanium irradiated at 13 MeV (for ^{68}Zn(p,n)^{68}Ga)				
^{48}V	0.525	191.09	[7,8]	1986.82
^{46}Sc	2.7529	0.83	[8]	1.74
75 µm thick niobium irradiated at 18 MeV (for ^{nat}Zn(p,n)^{61}Cu, and ^{64}Ni(p,n)^{64}Cu)				
^{93}Mo	48,000	345.13	[9]	0.023
^{92m}Nb	0.333	137.33	[8,10,11]	604.67
75 µm thick niobium irradiated at 13 MeV (for ^{68}Zn(p,n)^{68}Ga)				
^{93}Mo	48,000	1644.64	[9]	0.20
^{92m}Nb	0.333	8.01	[8,10,11]	126.12

Table 1. *Cont.*

Radioisotope Produced	Half-Life	Cumulated Production Yield	Cross-Section Data	Estimation of Activation after One Month of Irradiation
35 µm thick Havar® irradiated at 18 MeV (for $^{18}O(p,n)^{18}F$)				
^{184}Re	2.33	0.64	[12]	4.66
^{99}Tc	2.53×10^{6}	1.88	[13]	6.97×10^{-6}
^{95m}Tc	2.00	1.55	[8,14,15]	7.06
^{95}Nb	1.15	0.04	[8]	0.35
^{92m}Nb	0.333	0.031	[8]	0.37
^{59}Ni	9.12×10^{5}	181.80	[9]	1.87×10^{-3}
^{58}Co	2.328	214.86	[8,16–21]	847.82
^{57}Co	8.929	70.50	[8,17,21–26]	73.75
^{56}Co	2.537	43.72	[8,23]	158.58
^{55}Fe	32.84	110.15	[27,28]	31.46
^{54}Mn	10.26	14.13	[8,23,24,28–30]	12.88
^{51}Cr	0.910	148.06	[8,28,30]	1443.88
^{9}Be	1.745	0.06	[31–33]	0.32

The last column of Table 1 also presents an estimation of the activity produced for each of these radioisotopes after a period of one month, considering our particular routine schedule of irradiations. Since the half-lives considered are much larger than the time between consecutives irradiations, the decay between irradiations was neglected. For the few exceptions for which the half-life exceeds 2 weeks but is still less than the time unit considered—i.e. one month - (e.g., ^{48}V), a factor of 0.5 was applied as a rough approximation to account for the decay within the one-month duration. These monthly estimations were used to calculate the cumulative activity produced in the target windows, considering a 30-year-long operation cycle followed by another 30-year-long period of cooling as a practical example. The production and accumulation of radioactivity during this first 30-year cycle of routine production behaves similarly to an irradiation cycle, reaching saturation according to the half-life of the radioisotope in question, with the difference being that those calculations were conducted with a unit time of one month to make use of the monthly production yield calculated. The results obtained for the materials used as target windows are presented in Figure 1 and Table 2. It is possible to see that most of the overall activity resulting from such activation comes from Havar®, whereas niobium foils produced far less activation. Complementarily, Figure 2 enables us to have a closer look at the decay rates for these materials, confirming that Havar® is still the most relevant radioactive waste for the first decade of cooling time. Niobium only becomes relevant because of the presence of the long-lived ^{93}Mo, which is almost exclusively produced when irradiating niobium at 13 MeV (Table 1) and therefore almost avoided at larger initial energies.

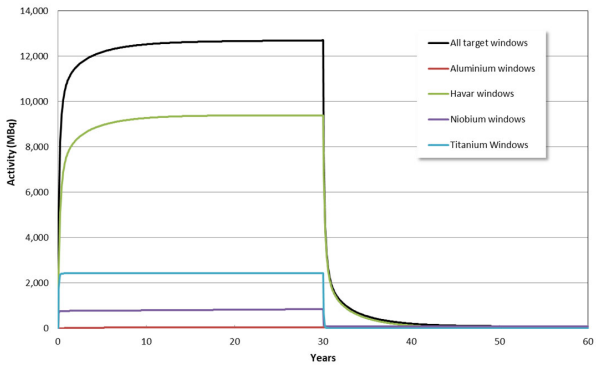

Figure 1. Activity present in the different target materials over time (initial 30 years of routine irradiations followed by 30 years of cooling time).

Table 2. Activity of the radioisotopes with half-lives greater than 2 weeks produced after 30 years of daily irradiations and after 30 years of cooling time.

	Radionuclide	Half-Life (Month)	Activity Produced after 30 Years of Daily Irradiations (MBq)	Residual Activity after 30 Years of Cooling Time (MBq)
Titanium	^{48}V	0.525	2388.1	0
	^{46}Sc	2.753	35.9	0
Niobium	^{93}Mo	48,000	80.1	79.7
	^{92m}Nb	0.333	763.2	0
Aluminium	^{22}Na	31.224	37.0	0.0125
	^{26}Al	8,604,000	0.0563	0.0563
Havar	^{9}Be	1.745	0.98	0
	^{51}Cr	0.910	2708.4	0
	^{54}Mn	10.260	197.2	0
	^{55}Fe	32.844	1505.5	0.755
	^{56}Co	2.537	663.4	0
	^{57}Co	8.929	987.4	0
	^{58}Co	2.328	3292.5	0
	^{59}Ni	912,000	0.67	0.67
	^{92m}Nb	0.333	0.42	0
	^{95}Nb	1.150	0.76	0
	^{95m}Tc	2.004	24.1	0
	^{99}Tc	2,533,200	0.0025	0.0025
	^{184}Re	1.248	10.9	0

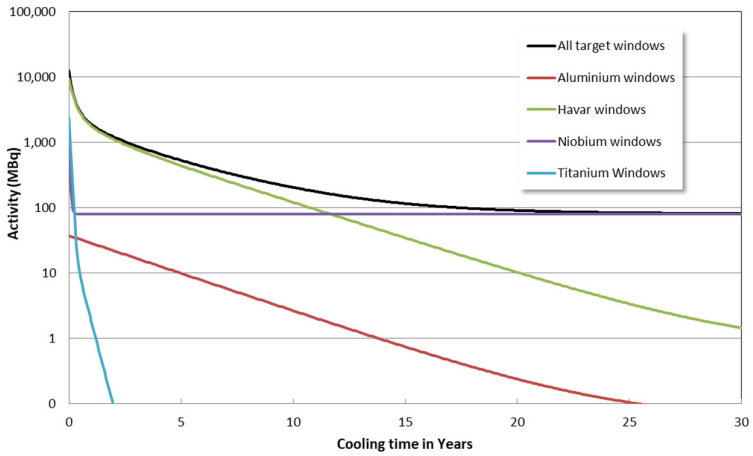

Figure 2. Activity present in the different target materials over a cooling period preceded by 30 years of routine irradiations.

Moreover, another relevant parameter to consider consists of the quantification of any radiocontaminants removed from the target window during irradiation and then transferred together with the irradiated liquid target. This is of particular interest as it can significantly affect the subsequent radiosynthesis. One of the most illustrative examples is the production of ^{68}Ga from liquid targets since the very sensitive radiolabeling conditions make the use of Havar forbidden [34,35]. Also, for the synthesis of ^{18}F-based compounds, the presence of radiometallic impurities was proven to affect the synthesis yields negatively [36,37]. Proofs of the non-negligible presence of these radiocontaminants rely on their accumulation in both the recovery vial for the irradiated enriched water and the QMA cartridge; therefore, they become long-term radioactive wastes. Figure 3 presents the high-purity germanium (HPGe) detector analysis performed on water irradiated under standard conditions for the production of ^{18}F using Havar® foil for 30 min. It shows that

the presence of the expected radiometalic contaminants actually increases with the aging of the Havar foil.

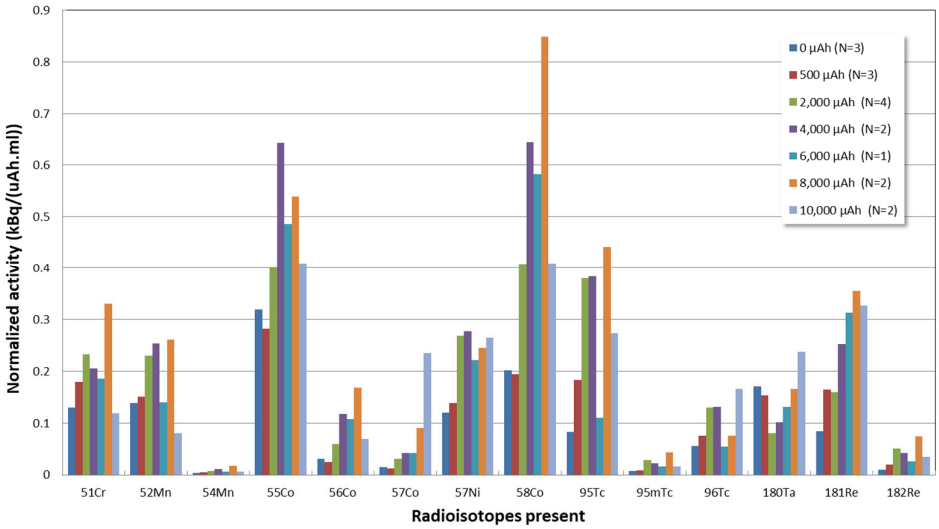

Figure 3. Activity measured for the radioisotopes present in the irradiated water when using Havar® foil as a function of the accumulated integrated target current in the foil (with N being the number of samples in each case).

The same occurs when producing ^{13}N with a Havar® window. In this case, these radiocontaminants are even present in the final product vial (FPV), albeit, naturally, in quantities far lower than those required to comply with the radionuclidic purity specification requirement of the European Pharmacopoeia [38]. Table 3 presents the activities of the radiometallic contaminant present in the FPV and confirms that the ageing of the Havar® target windows also results in increasing amounts of these contaminants.

Table 3. Radioisotopes present in the FPV of ^{13}N-NH_3 productions using a 35 µm thick Havar® foil as a target window.

Number of Runs since Installation of a New Havar® Target Foil	Activity (kBq)					
	^{52}Mn	^{55}Co	^{56}Co	^{57}Co	^{57}Ni	^{58}Co
1	0.170	0.335	0.051	n.d.	0.902	0.049
2	0.172	0.098	0.050	0.026	1.552	0.118
6	0.184	2.465	0.093	0.086	3.958	0.251
8	0.858	2.246	0.276	0.221	2.171	0.848
9	0.786	6.022	0.395	0.200	2.662	1.628
10	2.567	15.086	1.010	0.493	5.587	3.564
11	2.399	18.156	1.043	0.377	6.049	3.777
13	5.288	14.118	1.144	0.709	4.652	3.395
14	3.500	10.140	0.824	0.194	3.048	1.741
15	2.647	8.489	0.596	0.295	2.561	1.195
16	0.323	1.653	0.332	n.d.	3.856	0.250

Figure 4 presents gamma-spectrometry analysis performed with a HPGe detector on the FPV of ^{13}N-NH_3 productions using either 35 µm thick Havar® foil or 125 µm thick niobium foil as the target windows. The analysis was performed after a cooling period of more than 24 h to allow both ^{13}N and ^{18}F to decay. For this particular example of the production of ^{13}N, the thickness of niobium was increased to 125 µm so that the target window would simultaneously behave as a degrader (energy reduced down to 16.1 MeV [34]) in order to minimize the co-production of ^{15}O via the ^{16}O(p,pn)^{15}O reaction down to acceptable values. Target currents up to 40 µA are used with a consistent end-of-synthesis (EOS) yield at of 1.4 GBq/µAh (i.e., up to 20 GBq at EOS). Figure 4 shows that it is not possible to detect these radiometallic contaminants when using niobium, whereas these are easily detectable when using Havar® as the target window material.

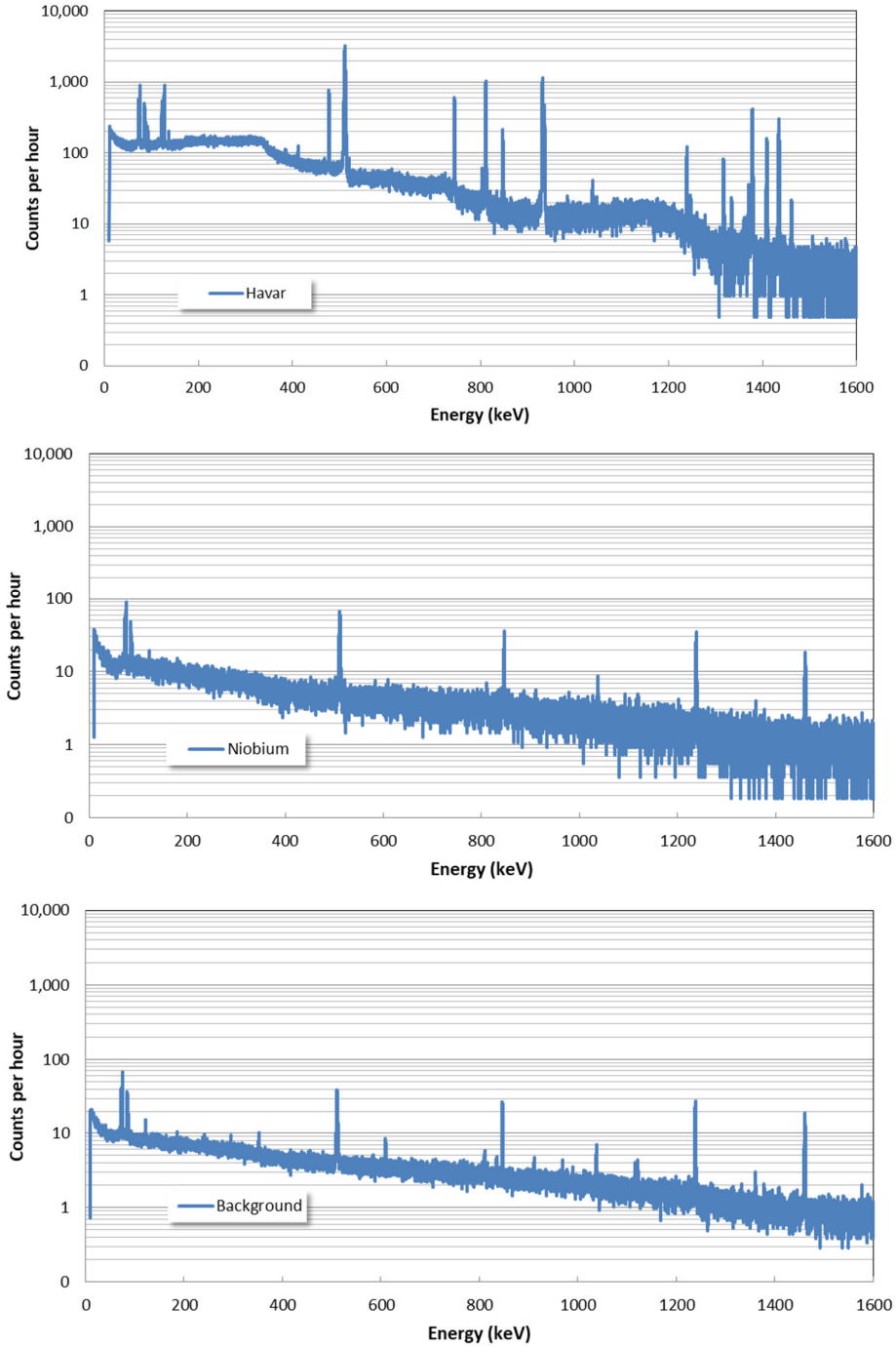

Figure 4. HPGe spectra of FPVs of ^{13}N-NH_3 productions after a 24 h cooling period when using either (i) a 35 µm thick Havar® foil (top) or (ii) a 125 µm thick niobium foil (middle) as target windows. (iii) A background spectrum (bottom) is also presented for direct comparison.

As previously demonstrated in [36,37], one can expect that the use of niobium windows would allow for an improvement in the yield of sensitive synthesis through the reduction of radiometallic contaminants. We unfortunately do not possess such proof so far as we still use Havar® for the production of ^{18}F. However, we already successfully implement niobium windows—with different thicknesses according to the production route—in most of our targets, i.e., not only in liquid targets developed for the production of radiometals (e.g., ^{68}Ga, ^{64}Cu, ^{61}Cu, ^{89}Zr) but also for the production of ^{13}N (Table 1). For instance, proton currents up to 75 µA are usually used for the production of ^{61}Cu [2], and currents of up to 90 µA are also successfully used when producing ^{68}Ga [39]. Our daily

experience shows that niobium can successfully be used as a material for target windows in daily, reliable irradiations, as long as the helium cooling system maintains its long-term stability and performance [39,40].

3. Conclusions

The several advantages of niobium—ranging from low activation to chemical inertness, among other examples—make it a suitable choice as a material for target windows. The only exception seems to be very large currents and/or pressures, for which Havar® remains the gold standard. Our calculations of material activation and the results of our comparison of the contamination of the irradiated transferred solutions prove our central claim. Moreover, our particular daily production routine has successfully demonstrated the potential of niobium as a material for target windows [2,39].

Author Contributions: Conceptualization, S.J.C.d.C. and F.A.; methodology, S.J.C.d.C. and F.A.; formal analysis, S.J.C.d.C. and F.A.; writing—original draft preparation, S.J.C.d.C.; writing—review and editing, S.J.C.d.C.; visualization, S.J.C.d.C.; supervision, F.A. All authors have read and agreed to the published version of the manuscript.

Funding: This research received no external funding.

Data Availability Statement: The original contributions presented in the study are included in the article, further inquiries can be directed to the corresponding author.

Conflicts of Interest: The authors declare no conflicts of interest.

References

1. IAEA RADIOISOTOPES AND RADIOPHARMACEUTICALS SERIES No.4 Cyclotron Produced Radionuclides: Operation and Maintenance of Gas and Liquid Targets. (n.d.). Cyclotron Produced Radionuclides: Operation and Maintenance of Gas and Liquid Targets | IAEA. Available online: https://www.iaea.org/publications/8783/cyclotron-produced-radionuclides-operation-and-maintenance-of-gas-and-liquid-targets (accessed on 21 May 2024).
2. Do Carmo, S.J.C.; Scott, P.J.H.; Alves, F. Production of radiometals in liquid targets. *EJNMMI Radiopharm. Chem.* **2020**, *5*, 154–196. [CrossRef]
3. Kajan, I.; Heinitz, S.; Kossert, K.; Sprung, P.; Dressler, R.; Schumann, D. First direct determination of the 93Mo half-life. *Sci. Rep.* **2021**, *11*, 19788. [CrossRef]
4. EXFOR Database-Experimental Nuclear Reaction Data. Available online: https://www.iaea.org/resources/databases/experimental-nuclear-reaction-data (accessed on 29 February 2024).
5. Hintzt, N.M.; Ramsey, N.F. D IFFERENTIAL n-P SCATTERING CROSS SECTION Excitation Functions to 100 Mev. *Phys. Rev.* **1952**, *88*, 19–27. [CrossRef]
6. Furukawa, M.; Shizuri, K.; Komura, K.; Sakamoto, K.; Tanaka, S. Production of 26Al and 22Na from proton bombardment of Si, Al and Mg. *Nucl. Phys.* **1971**, *174*, 539–544. [CrossRef]
7. West, H.I., Jr.; Lanier, R.G.; Mustafa, M.G. Excitation Functions for the Nuclear Reactions on Titanium Leading to the Production of 48V48V, 44Sc, and 47Sc by Proton, Deuteron and Triton Irradiations at 0–35 MeV, U.C., Lawrence Rad. Lab., Berkeley and Livermore 1993. Available online: https://digital.library.unt.edu/ark:/67531/metadc1314805/m2/1/high_res_d/10142277.pdf (accessed on 21 May 2024).
8. Levkovskij, V.N. Activation cross section nuclides of average masses (A = 40–100) by protons and alpha-particles with average energies (E = 10–50 MeV), Inter Vesi, Moscow, Russia. 1991. Available online: https://www-nds.iaea.org/CRP-CP-monitor/2RCM/Hussain-2RCM-2014.pdf (accessed on 21 May 2024).
9. Chodil, G.; Jopson, R.C.; Mark, H.; Swift, C.D.; Thomas, R.G.; Yates, M.K. (p,n) and (p,2n) cross sections of nine elements between 7.0 and 15.0 MeV. *Nucl. Phys.* **1967**, *93*, 648–672. [CrossRef]
10. Ditrói, F.; Hermanne, A.; Corniani, E.; Takács, S.; Tárkányi, F.; Csikai, J.; Shubin, Y.N. Investigation of proton induced reactions on niobium at low and medium energies. *Nucl. Instrum. Methods Phys. Res. Sect. B Beam Interact. Mater. At.* **2009**, *267*, 3364–3374. [CrossRef]
11. Avila-Rodriguez, M.A.; Wilson, J.S.; Schueller, M.J.; McQuarrie, S.A. Measurement of the activation cross section for the (p,xn) reactions in niobium with potential applications as monitor reactions. *Nucl. Instrum. Methods Phys. Res. Sect. B Beam Interact. Mater. At.* **2008**, *266*, 3353–3358. [CrossRef]
12. Lapi, S.; Mills, W.J.; Wilson, J.; McQuarrie, S.; Publicover, J.; Schueller, M.; Schyler, D.; Ressler, J.J.; Ruth, T.J. Production cross-sections of 181-186Re isotopes from proton bombardment of natural tungsten. *Appl. Radiat. Isot.* **2007**, *65*, 345–349. [CrossRef]

13. Gagnon, K.; Bénard, F.; Kovacs, M.; Ruth, T.J.; Schaffer, P.; Wilson, J.S.; McQuarrie, S.A. Cyclotron production of 99mTc: Experimental measurement of the 100Mo(p,x) 99Mo, 99mTc and 99gTc excitation functions from 8 to 18 MeV. *Nucl. Med. Biol.* **2011**, *38*, 907–916. [CrossRef]
14. Izumo, M.; Matsuoka, H.; Sorita, T.; Nagame, Y.; Sekine, T.; Hata, K.; Baba, S. Production of 95mTm with Proton Bombardment of 95Mo. *Int. J. Radiat. Appl. Instrumentation. Part A. Appl. Radiat. Isot.* **1991**, *42*, 297–301. [CrossRef]
15. Skakun, E.A.; Batij, V.G.; Rakivnenko, Y.N.; Rastrepin, O.A. Excitation Functions and Isomer Ratios for up-to-9-MeV Proton Interactions with Zr and Mo Isotope Nuclei. *Yad. Fiz.* **1987**, *46*, 28.
16. Alharbi, A.A.; Alzahrani, J.; Azzam, A. Activation cross-section measurements of some proton induced reactions on Ni, Co and Mo for proton activation analysis (PAA) purposes. *Radiochim. Acta* **2011**, *99*, 763–770. [CrossRef]
17. Schoen, N.C.; Orlov, G.; Mcdonald, R.J. (n.d.). Excitation functions for radioactive isotopes produced by proton bombardment of Fe, Co, and W in the energy range from 10 to 60 MeV. *Phys. Rev. C* **1979**, *20*, 88. [CrossRef]
18. Ghosh, R.; Badwar, S.; Lawriniang, B.; Jyrwa, B.; Naik, H.; Naik, Y.; Suryanarayana, S.V.; Ganesan, S. Measurement of Fe58(p,n)Co58 reaction cross-section within the proton energy range of 3.38 to 19.63 MeV. *Nucl. Phys. A* **2017**, *964*, 86–92. [CrossRef]
19. Sudar, S.; Szelecsenyi, F.; Qaim, S.M. Excitation function and isomeric cross-section ratio for the 'Ni(p, a) Co 'g process. *Phys. Rev. C* **1993**, *48*, 3115. [CrossRef]
20. Stearns, C.M. COMPARISON OF REACTIONS OF COPPER-63 COMPOUND NUCLEI FORMED BY ALPHA-PARTICLE, PROTON, AND CARBON-ION BOMBARDMENTS., EXFOR entry C237613, United States: N. p., 1962. Available online: https://www.osti.gov/biblio/4722126 (accessed on 21 May 2024).
21. Tanaka, S.; Furukawa, M.; Chibat, M. Nuclear reactions of nickel with protons up to 56 MeV. *J. Inorg. Nucl. Chem.* **1972**, *34*, 2419–2426. [CrossRef]
22. Ditrói, F.; Tárkányi, F.; Takács, S.; Hermanne, A.; Yamazaki, H.; Baba, M.; Mohammadi, A. Activation cross-sections of longer lived products of proton induced nuclear reactions on cobalt up to 70 MeV. *J. Radioanal. Nucl. Chem.* **2013**, *298*, 853–865. [CrossRef]
23. Wenrong, Z.; Hanlin, L.; Weixiang, Y. Measurement of cross sections by bombarding Fe with protons up to 19 MeV. *Chin. J. Nucl. Phys.* **1993**, *15*, 337–340.
24. Al-Abyad, M.; Comsan, M.N.H.; Qaim, S.M. Excitation functions of proton-induced reactions on ^{nat}Fe and enriched ^{57}Fe with particular reference to the production of 57Co. *Appl. Radiat. Isot.* **2009**, *67*, 122–128. [CrossRef]
25. Reimer, P.; Qaim, S.M. Excitation Functions of Proton Induced Reactions on Highly Enriched 58 Ni with Special Relevance to the Production of 55 Co and 57 Co. *Radiochim. Acta* **1998**, *80*, 113–120. [CrossRef]
26. Uddin, M.S.; Sudár, S.; Spahn, I.; Shariff, M.A.; Qaim, S.M. Excitation function of the Ni 60 (p,γ) Cu 61 reaction from threshold to 16 MeV. *Phys. Rev. C* **2016**, *93*, 044606. [CrossRef]
27. Jenkins, L.; Wain, A.G. Excitation functions for the bombardment of 56Fe with protons. *J. Inorg. Nucl. Chem.* **1970**, *32*, 1419–1425. [CrossRef]
28. Al-Abyad, M.; Spahn, I.; Qaim, S.M. Experimental studies and nuclear model calculations on proton induced reactions on manganese up to 45MeV with reference to production of 55Fe, 54Mn and 51Cr. *Appl. Radiat. Isot.* **2010**, *68*, 2393–2397. [CrossRef] [PubMed]
29. Michel, A.R.; Bodemann, R.; Busemann, H.; Dam, R.; Gloris, M.; Lange, H.; Klug, B.; Krins, A.; Leya, I.; Liipke, M.; et al. Cross sections for the production of residual nuclides by low-and medium-energy protons from the target elements C, N, O, Mg, Al, Si, Ca, Ti, V, Mn, Fe, Co, Ni, Cu, Sr, Y, Zr, Nb, Ba and Au. *Nucl. Instrum. Methods Phys. Res. Sect. B: Beam Interact. Mater. At.* **1997**, *129*, 153–193. [CrossRef]
30. Ditrói, F.; Tárkányi, F.; Takács, S.; Hermanne, A.; Yamazaki, H.; Baba, M.; Mohammadi, A. Activation cross-sections of longer lived products of proton induced nuclear reactions on manganese up to 70 MeV. *Nucl. Instrum. Methods Phys. Res. Sect. B Beam Interact. Mater. At.* **2013**, *308*, 34–39. [CrossRef]
31. Cohen, B.I.; Handley, T.H. Experimental Studies of (p, t) Reactions. *Phys. Rev.* **1954**, *93*, 514–517. [CrossRef]
32. Hermanne, A.; Tarkanyi, F.; Takacs, S. Activation cross sections for production of 7Be by proton and deuteron induced reactions on 9Be: Protons up to 65MeV and deuterons up to 50MeV. *Appl. Radiat. Isot.* **2014**, *90*, 203–207. [CrossRef]
33. Inoue, T.; Tanaka, S. Production of 7Be from proton bombardment of light elements. *J. Inorg. Nucl. Chem.* **1976**, *38*, 1425–1427. [CrossRef]
34. Alves, F.; Alves, V.H.; Neves, A.C.B.; do Carmo, S.J.C.; Nactergal, B.; Hellas, V.; Kral, E.; Gonçalves-Gameiro, C.; Abrunhosa, A.J. Cyclotron production of Ga-68 for human use from liquid targets: From theory to practice. *AIP Conf. Proc.* **2017**, *1845*, 020001. [CrossRef]
35. Alves, F.; Alves, V.H.P.; do Carmo, S.J.C.; Neves, A.C.B.; Silva, M.; Abrunhosa, A.J. Production of copper-64 and gallium-68 with a medical cyclotron using liquid targets. *Mod. Phys. Lett. A* **2017**, *32*, 1740013. [CrossRef]
36. Wilson, J.S.; Avila-Rodriguez, M.A.; Johnson, R.R.; Zyuzin, A.; McQuarrie, S.A. Niobium sputtered Havar foils for the high-power production of reactive [18F]fluoride by proton irradiation of [18O]H2O targets. *Appl. Radiat. Isot.* **2008**, *66*, 565–570. [CrossRef] [PubMed]
37. Gagnon, K.; Wilson, J.S.; Sant, E.; Backhouse, C.J.; McQuarrie, S.A. Assessing the performance and longevity of Nb, Pt, Ta, Ti, Zr, and ZrO 2-sputtered Havar foils for the high-power production of reactive [18F]F- by proton irradiation of [18O]H 2O. *Appl. Radiat. Isot.* **2011**, *69*, 1330–1336. [CrossRef] [PubMed]

38. Ammonia (13N) Injection. *European Pharmacopoia*; 10.0; EDQM: Strasbourg, France, 2019; p. 1183.
39. Do Carmo, S.J.C.; Kral, E.; Geets, J.-M.; Nactergal, B.; Abrunhosa, A.; Alves, F. Improved production of novel radioisotopes with custom energy Cyclone® Kiube. *Instruments* **2024**. *submitted for publication*.
40. Do Carmo, S.J.C.; de Oliveira, P.M.; Alves, F. Thermal simulation studies for the characterization of a cyclotron liquid target with thick niobium target windows. *Appl. Sci.* **2021**, *11*, 10922. [CrossRef]